



Light curve parametrization of three rice (*Oryza sativa* L.) cultivars based on mechanistic models

Z.P. YE^{*†}, S.X. ZHOU^{**†}, X.L. YANG^{***}, H.J. KANG[#], S.H. DUAN^{###,+}, and F.B. WANG^{*,+}

*Maths & Physics College, Jinggangshan University, 343009 Ji'an, China**

*The New Zealand Institute for Plant and Food Research Limited, 4130 Hawke's Bay, New Zealand***

*School of Life Sciences, Nantong University, Nantong, 226019 Jiangsu, China****

Wenzhou Vocational College of Science & Technology, 325006 Wenzhou, China#

School of Life Sciences, Jinggangshan University, 343009 Ji'an, China###

Abstract

This study aimed to assess variations in leaf gas-exchange characteristics, leaf pigment contents, and some intrinsic traits of photosynthetic pigment molecules in three rice cultivars (cv. JR3015, Wufengyou3015, and Jifengyou3015) using mechanistic models. The findings revealed that chlorophyll content varied significantly among the three cultivars, but not maximum electron transport rate. JR3015 had lower chlorophyll content but the highest eigen-absorption cross-section (σ_{ik}) and the lowest minimum average life-time of photosynthetic pigment molecules in the excited state (τ_{min}). Our results suggested that the highest σ_{ik} and the lowest τ_{min} in JR3015 facilitated its electron transport rate despite its lower leaf chlorophyll content. Furthermore, compared to Jifengyou3015 and Wufengyou3015, JR3015 had the lowest photosynthetic electron-use efficiency *via* PSII, which contributed to its lowest maximum net photosynthetic rate. These findings are important in selecting rice cultivars based on their differences in photosynthetic capacity.

Keywords: minimum average lifetime; *Oryza sativa* L.; photosynthesis; photosynthetic light-response curve; photosynthetic pigment molecules.

Highlights

- Contrary to J_{max} , chlorophyll contents and P_{Nmax} differed between the three rice cultivars
- Despite lower pigment, JR3015 matches J_{max} of others due to higher σ_{ik} and lower τ_{min}
- JR3015's lowest θ resulted in its lowest P_{Nmax} compared to other rice cultivars

Received 9 March 2024

Accepted 5 September 2024

Published online 30 September 2024

[†]Corresponding author

e-mail: wangfubiao@jgsu.edu.cn

shihua_duan@aliyun.com

Abbreviations: d – thickness of leaf sample; g_i and g_k – degeneracy of energy level of photosynthetic pigment molecules in the ground state (i) and excited state (k); I – light intensity; I_c – light-compensation point; I_{sat} – saturation light intensity corresponding to maximum net photosynthetic rate; J – electron transport rate; $J-I$ – light-response curve of photosynthetic electron transport rate; J_{max} – maximum photosynthetic electron transport rate; n_0 – number of photosynthetic pigment molecules of the measured leaf sample per unit volume; N_0 – total photosynthetic pigment molecules of the measured leaf sample; N_k – numbers of photosynthetic pigment molecules in the excited state k ; PAR_{sat} – saturation irradiance corresponding to maximum electron transport rate; P_N – net photosynthetic rate; P_N-I – light-response curve of photosynthesis; P_{Nmax} – maximum net photosynthetic rate; R_d – mitochondrial CO_2 release in the dark; S – measured area of leaf sample; α' – fraction of light absorbed by PSII; α_s – slope of linear part of light response curve in weak photosynthetic flux density between 0 and $150 \mu\text{mol}(\text{photon}) \text{m}^{-2} \text{s}^{-1}$; α_c – initial slope of light response curve of electron transport rate; α_p – initial slope of photosynthesis–irradiance response; β' – leaf absorptance; β_c – coefficient of dynamic downregulation for PSII/photoinhibition of light-response curve of photosynthetic electron transport rate; β_p – coefficient of dynamic downregulation for PSII/photoinhibition of light-response curve of photosynthesis; γ_c – saturation coefficient of light-response curve of photosynthetic electron transport rate; γ_p – saturation coefficient of light-response curve of photosynthesis; θ – electron-use efficiency *via* PSII; σ_{ik} – eigen-absorption cross-section of photosynthetic pigment molecule from ground state i to excited state k due to light illumination; τ_{min} – minimum average lifetime of photosynthetic pigment molecules in the excited state; ϕ – exciton-use efficiency in PSII.

Acknowledgments: This research was supported by the Natural Science Foundation of China (Grant No. 32260063 and 32060428), the Natural Science Foundation of Jiangxi Province (Grant No. 20224BAB205020), and the Project Funded by Jiangxi Provincial Department of Education (Grant No. GJJ201036).

[†]These authors have contributed equally to this work.

Conflict of interest: The authors declare that they have no conflict of interest.

Introduction

Light energy is a fundamental driving factor in the process of photosynthesis in plant leaves. In higher plants, photosynthetic pigment molecules absorb the light energy, which is then resonantly transferred to neighboring pigment molecules and ultimately to the reaction center, where it drives primary charge separation (Kondo *et al.* 2017, Mirkovic *et al.* 2017). During this process, the absorbed light energy is mostly utilized for photochemistry, while a portion of it is dissipated as heat dissipation and chlorophyll fluorescence (Roháček 2002). However, when light energy exceeds the amounts required for photochemistry, and the photosynthetic electrons cannot be transferred efficiently (Sanda *et al.* 2011), the excess light energy can cause damage to the photosynthetic apparatus (Yang *et al.* 2023). To alleviate or avoid such damage, the excess energy can be dissipated *via* heat emission, which is linked to changes in the conversion state of the xanthophyll cycle and an increase in nonphotochemical quenching of fluorescence (NPQ) (Zhao *et al.* 2017). This mechanism protects the photosynthetic apparatus and enables plants to avoid oxidative stress (Sofó *et al.* 2009, Nilkens *et al.* 2010, Essemine *et al.* 2017, Zhao *et al.* 2017). Chlorophylls are essential components of chloroplasts that play a vital role in light capture and energy transduction (Hu *et al.* 2018, Yang *et al.* 2020a). The adaptation of the photosynthetic apparatus to high levels of irradiance is crucial for plant survival and growth (Ruban 2015, Silva *et al.* 2018).

The relationship between leaf photosynthesis and leaf chlorophyll content has been extensively researched in the field of plant science (Chen 2014, Li *et al.* 2018, Chen *et al.* 2019, Hitchcock *et al.* 2022, Hu *et al.* 2023). Numerous studies have demonstrated a positive correlation between chlorophyll content and photosynthetic capacity in various plant species, including rice (Chen 2014, Chen *et al.* 2019, Hitchcock *et al.* 2022, Hu *et al.* 2023), wheat (Qian *et al.* 2021), hybrid poplar (Coleman *et al.* 2008, Chandra and Kang 2016), subterranean clover (Mauro *et al.* 2011), soybean (Slattery *et al.* 2017), and twenty-two common British angiosperms (Murchie and Horton 2008). These findings suggest an association between higher chlorophyll content and increased photosynthesis. However, some studies have reported a negative relationship or no correlation between the two (Tekalign and Hammes 2004, Murchie and Horton 2008, Insausti 2015, Chandra and Kang 2016, Kalisz *et al.* 2016, Slattery *et al.* 2017, Zhao *et al.* 2021). For example, during the process of ethylene-induced leaf senescence, although the chlorophyll content in the quick-leaf-senescence inbred line of maize (*Zea mays* L.) decreases faster than that of the stay-green inbred line, its photosynthetic capacity is greater than the latter (Zhang *et al.* 2012). These results suggest that congeneric plant taxa can exhibit either low leaf chlorophyll content but high photosynthetic capacity or high leaf chlorophyll content but low photosynthetic capacity (Zhang *et al.* 2012, Chen 2014, Chen *et al.* 2019). The conflicting results have led to controversy regarding the impact of photosynthetic pigment molecules on

electron transport rate and CO₂ assimilation (Qian *et al.* 2021). The mechanisms underlying these differences are not well understood in terms of light energy absorption by photosynthetic pigment molecules among closely related plant taxa.

Research on the effective utilization of light energy by plants with low leaf chlorophyll content under normal light conditions has primarily focused on patterns of light energy allocation and utilization (Hussain *et al.* 2019), photosynthetic enzyme activity and regulatory mechanisms (Qian *et al.* 2021), as well as leaf structure and function (Chen *et al.* 2019, Hitchcock *et al.* 2022). However, further investigation is required to uncover the specific characteristics of chlorophyll pigment molecules in plants with low leaf chlorophyll content and their relation to light absorption and adaptation strategies. The present study posits that plant taxa with low leaf chlorophyll content may exhibit specific adaptive characteristics in light absorption. Specifically, our hypotheses are as follows: first, the eigen-absorption cross-section of photosynthetic pigment molecules (σ_{ik} ; see Appendix 1 for the list of abbreviations) in plants with low chlorophyll content may be higher, allowing these plants to absorb more light energy under high levels of irradiance; second, the lower numbers of photosynthetic pigment molecules in the lowest excited state (N_k) in these plants could enhance light absorption, and their shorter minimum average lifetime of photosynthetic pigment molecules (τ_{\min}) may facilitate the transfer of excited energy to photochemical reactions; lastly, the consumption of photosynthetic electrons in these plants to assimilate one CO₂ molecule may be higher, which could enhance the electron transport rate but at the cost of a lower net photosynthetic rate (P_N).

To test these hypotheses, we experimented on three rice cultivars to examine the properties of photosynthetic pigment molecules in light energy absorption, the excited energy transfer, and the utilization of light energy, as well as the attributes of photosynthetic pigment molecules. These findings offer valuable insights into the fundamental processes of photosynthesis and have the potential to aid in the development of rice varieties with higher light efficiency, thereby increasing food production.

Materials and methods

Plant materials: Seeds of three rice cultivars, *i.e.*, JR3015, Wufengyou3015, and Jifengyou3015 accessions, were provided by the Rice Research Institute of Jiangxi Academy of Agricultural Sciences. Among the three rice cultivars, JR3015 is a restorer line, and the other two rice cultivars are F1 hybrid of JR3015, which have high photosynthetic capacity both at tillering and heading stages. Rice seeds were placed within Petri plates on two layers of *Whatman No. 5* filter paper and rinsed with 7 mL of carbendazim (0.025% w/v) under ambient temperature conditions (26°C) in the dark until the emergence of the radicle. At the four-leaf stage, the plants were transferred into thirty plastic pots and put in the field in the Botanical Garden of Jinggangshan University. The potted soil was taken from the rice field, with 5 kg of soil per plastic

pot. The amount of fertilizer applied to each pot was equivalent to the conventional field application, which means 0.3 g of nitrogen, 0.12 g of phosphorus pentoxide, and 0.21 g of potassium oxide were applied to each pot. When fertilizing, the amounts of nitrogen, phosphorus, and potassium applied to each pot were converted into the corresponding fertilizers so that the content of these three elements matched the content found in urea, calcium dihydrogen phosphate, and potassium chloride, respectively. The phosphorus and potassium fertilizers were applied as base fertilizers once, while nitrogen was applied in two stages as a base fertilizer and as a top dressing for tillering, in a ratio of 60:40 (%). The pots were maintained with a shallow layer of water throughout the entire rice growth period. Timely prevention and control measures were taken against diseases and pests. Mature, healthy, and non-senescent flag leaves from 6- to 7-week-old plants were used for our measurements. There were three repeated measurements per cultivar.

Gas-exchange measurements: Net CO₂ assimilation rate (P_N) and chlorophyll *a* fluorescence were measured on the same leaf area (4 cm²) of the flag leaves in the dough stage. Five plants per rice cultivar were used to measure simultaneously their gas exchange and chlorophyll fluorescence. A portable photosynthesis system (*Li-Cor*, Lincoln, NE, USA) coupled with an integrated fluorometer chamber head (*LI-6400-40*, *Li-Cor*, Lincoln, NE, USA) was used for gas-exchange and chlorophyll fluorescence measurements. All measurements were performed between 9:00 and 16:00 h. The gas-exchange system allowed control of CO₂ concentration at 390 μmol mol⁻¹ by an integrated CO₂ mixer (*LI-6400-01*, *Li-Cor*, Lincoln, NE, USA), and the flow rate was adjusted to 400 μmol s⁻¹. Leaf temperatures ranged from 30.5 to 31.5°C. The relative humidity was adjusted to 60–70% using a dew-point generator (*LI-610*, *Li-Cor*). Leaves were acclimated to natural irradiance of 2,000 μmol(photon) m⁻² s⁻¹ for 30 min at 9:30 h on sunny days. Both light-response curve of net CO₂ assimilation rates (P_N-I) and of electron transport rate ($J-I$) measurements were simultaneously conducted in accordance to a descending order of irradiance levels: 2,000; 1,800; 1,600; 1,400; 1,200; 1,000; 800; 600; 400; 200; 100; 50 and 0 μmol(photon) m⁻² s⁻¹. Data were manually logged when the gas-exchange parameter became stable. The lowest and highest values were excluded, and the three best biological replicates were used for the subsequent curve fitting and parameter calculations. The P_N-I and $J-I$ curves were simulated using the two models we developed previously (Ye *et al.* 2013a,b), with the P_N-I curve being accurately represented by Eq. 1:

$$P_N = \alpha_p \frac{1 - \beta_p I}{1 + \gamma_p I} I - R_d \quad (1)$$

where P_N is the net photosynthetic rate, α_p is the initial slope of the P_N-I curve, β_p is referred to as the coefficient of dynamic downregulation for PSII/photoinhibition of the light-response curve of photosynthesis, γ_p is referred to as the saturation coefficient of the light-response curve

of photosynthesis, R_d is the dark respiratory rate (Ye *et al.* 2013a,b).

The saturation irradiance (I_{sat}) corresponding to the maximum net photosynthetic rate ($P_{N\text{max}}$) can be calculated according to the following equations:

$$I_{\text{sat}} = \frac{\sqrt{(\beta_p + \gamma_p)/\beta_p} - 1}{\gamma_p} \quad (2)$$

$$P_{N\text{max}} = \alpha_p \left(\frac{\sqrt{\beta_p + \gamma_p} - \sqrt{\beta_p}}{\gamma_p} \right)^2 - R_d \quad (3)$$

The $J-I$ curves were simulated with Eq. 4 (Ye *et al.* 2013a,b):

$$J = \alpha_e \frac{1 - \beta_e I}{1 + \gamma_e I} I \quad (4)$$

where J is the electron transport rate, α_e is the initial slope of the $J-I$ curve, β_e is referred to as the coefficient of dynamic downregulation for PSII/photoinhibition of the light-response curve of photosynthetic electron transport rate, γ_e is referred to as the saturation coefficient of the light-response curve of photosynthetic electron transport rate (Ye *et al.* 2013a,b).

The saturation irradiance (PAR_{sat}) corresponding to the maximum electron transport rate (J_{max}) can be calculated by the following equations:

$$\text{PAR}_{\text{sat}} = \frac{\sqrt{(\beta_e + \gamma_e)/\beta_e} - 1}{\gamma_e} \quad (5)$$

$$J_{\text{max}} = \alpha_e \left(\frac{\sqrt{\beta_e + \gamma_e} - \sqrt{\beta_e}}{\gamma_e} \right)^2 \quad (6)$$

When chlorophyll content [mg m⁻²] is quantified, σ_{ik} can be calculated as follows (Ye *et al.* 2013a,b):

$$\sigma_{\text{ik}} = \frac{S \alpha_e}{\alpha' \beta' \phi N_0} = \frac{\alpha_e}{\alpha' \beta' \phi n_0 d} \quad (7)$$

where S is the measured area of leaf sample [m²], α' is fraction of light absorbed by PSII (dimensionless), β' is leaf absorptance (dimensionless), ϕ is the exciton-use efficiency in PSII (dimensionless), N_0 is total photosynthetic pigment molecules of the measured leaf sample, n_0 is the number of photosynthetic pigment molecules of the measured leaf sample per unit volume [m⁻³], and d is the thickness of leaf sample [m].

According to Ye *et al.* (2013a,b), the numbers of photosynthetic pigment molecules in the excited state k (N_k) and minimum average lifetime of photosynthetic pigment molecules in the excited state (τ_{min}) can be calculated by the following equations:

$$N_k = \frac{1}{1 + g/g_k} \frac{\gamma_e I}{1 + \gamma_e I} N_0 \quad (8)$$

$$\tau_{\text{min}} > \frac{0.03 \gamma_e}{(1 + g/g_k) \sigma_{\text{ik}}} \quad (9)$$

where g_i and g_k are the degeneracy of the energy level of photosynthetic pigment molecules in the ground state (i) and excited state (k) (dimensionless), respectively. The biological significance of other parameters is the same as in other equations.

All key quantitative traits (*e.g.*, α_e , PAR_{sat} , J_{max} , σ_{ik} , N_k , and τ_{min} from the $J-I$ curve; α_p , P_{Nmax} , I_{sat} , I_c , and R_d from the P_N-I curve) were calculated using the *Photosynthesis Model Simulation Software (PMSS)*, Jिंगgangshan University, Ji'an, China) (<http://photosynthetic.sinaapp.com>).

Photosynthetic pigments: To determine the chlorophyll content, 100 mg of chopped leaf samples were placed in capped measuring tubes containing 25 mL of 80% acetone and kept inside a refrigerator (4°C) for 48 h (Sarkar 1997). The extract was centrifuged at a speed of $6,000 \times g$ at 4°C for 5 min. The chlorophyll content per unit leaf area was measured spectrophotometrically by taking optical density at 663.6 and 646.6 nm (Lichtenthaler 1987, Porra 2002). The concentrations of chlorophyll *a* (Chl *a*), chlorophyll *b* (Chl *b*), and total chlorophyll were calculated according to the following formulas (Lichtenthaler 1987):

$$\text{Chl } a \text{ [mg L}^{-1}\text{]} = 12.25A_{663.6} - 2.55A_{646.6} \quad (10)$$

$$\text{Chl } b \text{ [mg L}^{-1}\text{]} = 20.31A_{646.6} - 4.91A_{663.6} \quad (11)$$

$$\text{Chl } (a+b) \text{ [mg L}^{-1}\text{]} = \text{Chl } a + \text{Chl } b \quad (12)$$

Statistical analysis: All variables are expressed as mean values (\pm SE) from three samples ($n = 3$) for each rice cultivar. Results were subjected to a one-way analysis of variance (ANOVA). *Student's t*-test was employed to test whether there were significant differences in fitted values among different rice cultivars at the 5% level of significance ($p < 0.05$) by using the statistical package *SPSS 18.5* statistical software (SPSS, Chicago, IL). Goodness of fit of the mathematical models to experimental data was assessed using the coefficient of determination (R^2).

Results

Difference in J , P_N , and fluorescence parameters of the three rice cultivars, and their response characteristics to irradiance:

The J rapidly increased with irradiance below about $600 \mu\text{mol}(\text{photon}) \text{m}^{-2} \text{s}^{-1}$, gradually reaching a peak. Beyond saturation irradiance, J decreased due to photoinhibition (Fig. 1). The three rice cultivars showed similar shapes of curves, with a remarkable region of photoinhibition occurring at $I > PAR_{sat}$. There were no significant differences in J_{max} and PAR_{sat} among the studied cultivars. The τ_{min} of rice cultivars Jifengyou3015 and Wufengyou3015 were significantly higher than that of JR3015, while the σ_{ik} of rice cultivar JR3015 was significantly higher than those of Jifengyou3015 and Wufengyou3015. The initial slopes of light-response curves of electron transport rate (α_e) did not show significant differences between the three rice cultivars. Table 1 presents the chlorophyll physical parameters (*e.g.*, σ_{ik} and τ_{min}) calculated using equations based

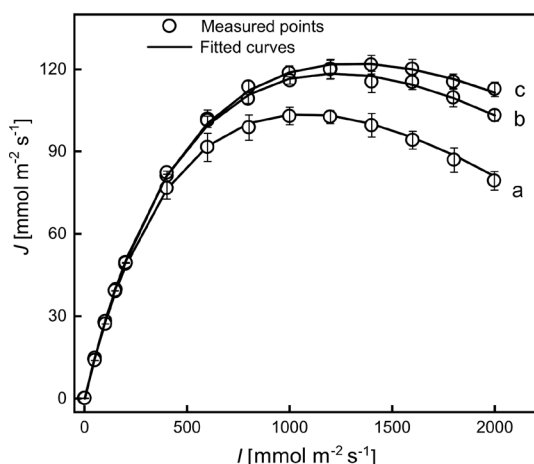


Fig. 1. Light-response curves of electron transport rate for three rice species (a – JR3015; b – Wufengyou3015; and c – Jifengyou3015). Values are means \pm standard errors ($n = 3$). J – electron transport rate; I – light intensity.

on our previous studies (Ye *et al.* 2013a,b), alongside the estimated primary chlorophyll fluorescence parameters (*i.e.*, J_{max} and PAR_{sat}). It is worth emphasizing that the estimated J_{max} and PAR_{sat} are in very close agreement with the measured data, exhibiting no significant difference (Fig. 1 and Table 1, $R^2 > 0.994$).

Similarly, P_N gradually increased with irradiance until it reached the saturation level for the rice cultivars Jifengyou3015 and Wufengyou3015. However, for JR3015, P_N declined significantly beyond the saturation irradiance (Fig. 2). Both P_{Nmax} and I_{sat} of the Jifengyou3015 cultivar were significantly higher than those of other cultivars. For instance, the Jifengyou3015 cultivar exhibited P_{Nmax} values of $26.30 \mu\text{mol} \text{m}^{-2} \text{s}^{-1}$ and I_{sat} values of $1,771.08 \mu\text{mol}(\text{photon}) \text{m}^{-2} \text{s}^{-1}$, respectively (Table 2). The JR3015 cultivar showed photoinhibition (a remarkable decline of P_N-I curve at $I > I_{sat}$) beginning above the lower value of I_{sat} about $1,200 \mu\text{mol}(\text{photon}) \text{m}^{-2} \text{s}^{-1}$ than those of Jifengyou3015 and Wufengyou3015. However, the I_{sat} value of approximately $1,800 \mu\text{mol}(\text{photon}) \text{m}^{-2} \text{s}^{-1}$ for Jifengyou3015 indicated that this cultivar still absorbed light energy and CO_2 for photosynthesis even under high-level irradiance (Fig. 2, Table 2). To compare PAR_{sat} and I_{sat} , we found that CO_2 assimilation did not reach synchronous saturation with the electron transport rate for the rice cultivars.

The values of J were further considered alongside those of P_N to evaluate θ ($\theta = \alpha_p/\alpha_e$), where higher values of θ indicate higher electron-use efficiency. The reciprocal of θ ($1/\theta$) suggests that the assimilation of one CO_2 molecule requires a certain number of electrons to be consumed. The reciprocal of θ_a [where $\theta_a = \alpha_a/\alpha_e$, and α_a represents apparent quantum yield, which is the slope of the linear part of the light response curve in weak photosynthetic flux density (PFD) between 0 and $150 \mu\text{mol}(\text{photon}) \text{m}^{-2} \text{s}^{-1}$] indicates that the assimilation of one CO_2 molecule requires apparent electrons numbers. In this study, electron numbers consumed per assimilation of a CO_2 molecule for the rice cultivar JR3015 were higher than

Table 1. Fitted values of key fluorescence parameters (α_e , PAR_{sat} , J_{max} , σ_{ik} , and τ_{min}), derived from $J-I$ curves according to a mechanistic model (Ye *et al.* 2013b) for three rice cultivars. The parameters are: initial slope of light-response curve of electron transport rate (α_e , [$\mu\text{mol } \mu\text{mol}^{-1}$]), maximum electron transport rate (J_{max} , [$\mu\text{mol m}^{-2} \text{s}^{-1}$]), saturation irradiance (PAR_{sat} , [$\mu\text{mol m}^{-2} \text{s}^{-1}$]), chlorophyll content (Chl ($a+b$), [g m^{-2}]), ratio of chlorophyll a and chlorophyll b (Chl $a/\text{Chl } b$), eigen-absorption cross-section of photosynthetic pigment molecule from ground state i to excited state k due to light illumination (σ_{ik} , [10^{-21} m^2]), minimum average life-time of photosynthetic pigments in the excited state (τ_{min} , [10^{-3} s]), and determination coefficient (R^2). All values indicate the mean \pm SE ($n = 3$) except for the measured values. Significant differences of three rice cultivars are indicated by *lowercase letters* ($p < 0.05$).

	JR3015		Wufengyou3015		Jifengyou3015	
	Fitted values	Measured values	Fitted values	Measured values	Fitted values	Measured values
α_e [$\mu\text{mol } \mu\text{mol}^{-1}$]	0.321 ± 0.00^a	-	0.323 ± 0.010^a	-	0.319 ± 0.007^a	-
J_{max} [$\mu\text{mol m}^{-2} \text{s}^{-1}$]	104.01 ± 9.08^a	≈ 102.97	114.05 ± 3.03^a	≈ 112.49	122.33 ± 6.91^a	≈ 121.97
PAR_{sat} [$\mu\text{mol m}^{-2} \text{s}^{-1}$]	$1,025.07 \pm 57.58^a$	$\approx 1,000$	$1,273.99 \pm 75.88^a$	$\approx 1,200$	$1,307.97 \pm 37.41^a$	$\approx 1,200$
Chl ($a+b$) [g m^{-2}]	-	0.320 ± 0.052^b	-	0.552 ± 0.055^a	-	0.558 ± 0.011^a
Chl $a/\text{Chl } b$	-	2.39 ± 0.04^a	-	2.36 ± 0.10^a	-	2.40 ± 0.02^a
σ_{ik} [10^{-21} m^2]	3.95 ± 0.13^a	-	2.33 ± 0.11^b	-	2.26 ± 0.09^b	-
τ_{min} [10^{-3} s]	9.42 ± 1.33^b	-	15.81 ± 1.59^a	-	14.24 ± 1.78^a	-
R^2	0.995 ± 0.001	-	0.997 ± 0.001	-	0.998 ± 0.001	-

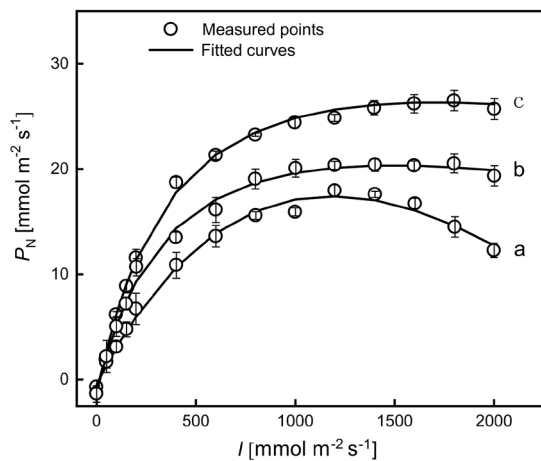


Fig. 2. Light-response curves of photosynthesis for three rice species (a – JR3015; b – Wufengyou3015; and c – Jifengyou3015). Values are means \pm standard errors ($n = 3$). P_N – net photosynthetic rate; I – light intensity.

those for the other cultivars. This means that the electron-use efficiency for JR3015 was the lowest among the three rice cultivars. However, the rice cultivars Jifengyou3015 and Wufengyou3015 did not differ significantly in $1/\theta$ despite the significant difference in their P_{Nmax} (Table 2). No significant differences were observed in $1/\theta_a$ among the three rice cultivars (Table 2). Additionally, the estimated main photosynthetic parameters (*e.g.*, I_{sat} , P_{Nmax} , I_c , and R_d) are in very close agreement with the measured data, showing no significant difference (Table 2, $R^2 > 0.984$).

Intrinsic physical parameters of photosynthetic pigment molecules and their responses to irradiance: When light illuminates a plant leaf, photosynthetic pigment molecules within the chloroplasts absorb it, exciting the pigment molecules from the ground state (state i) to a low excitation state (state k). Light-driven changes in the numbers of the photosynthetic pigment molecules in the lowest

excited state (N_k) were determined for each rice cultivar by Eq. 8 (Ye *et al.* 2013b) (Fig. 3). The N_k of JR3015 was significantly lower than that of other rice cultivars, while the N_k of Wufengyou3015 and Jifengyou3015 did not differ significantly. A rapid increase in N_k with increased I was observed in both Wufengyou3015 and Jifengyou3015, which incidentally exhibited higher values for PAR_{sat} , and had a knock-on effect on J_{max} and P_{Nmax} , possibly due to their capability of transferring more excitons to photochemistry and producing increased photosynthetic electron flow. The rate of N_k increase with increasing I was similar for Wufengyou3015 and Jifengyou3015, reflecting their similar trends of J vs. I .

Discussion

Leaf photosynthesis and physical parameters of photosynthetic pigment molecules: The initial slope of the light-response curve of the electron transport rate [α_e , $\mu\text{mol}(\text{electron}) \mu\text{mol}^{-1}(\text{photon})$] is frequently interpreted as an indicator of light energy conversion into photosynthetic electron flow (Ye *et al.* 2013a,b; Chen *et al.* 2021). In general, species exhibiting a steeply sloping curve should be capable of higher electron transport rates at low light levels compared to those with a less steeply sloping curve (Ye *et al.* 2020, Kitao *et al.* 2021). In this study, three rice cultivars exhibited no significant difference in α_e values (Table 1); however, both J_{max} and PAR_{sat} values of Jifengyou3015 and Wufengyou3015 were significantly higher than those of JR3015. Despite the chlorophyll content of JR3015 being nearly half that of Jifengyou3015 and Wufengyou3015, its J_{max} value was 0.86 and 0.92 times those of Jifengyou3015 and Wufengyou3015, respectively. This contradictory pattern may be attributed to specific differences in the number of chlorophyll reaction centers per unit area among cultivars (Major and Dunton 2002). Chlorophyll is an important component of the chloroplast that serves as the fundamental basis for leaf photosynthesis (Silva *et al.* 2018). Additionally, it is an essential indicator

Table 2. Fitted values of key photosynthetic parameters (α_p , $1/\theta$, I_{sat} , P_{Nmax} , I_c , and R_d), derived from P_N-I curves according to a mechanistic model (Ye *et al.* 2013b) for three rice cultivars. The parameters are: initial slope of light-response curve of photosynthesis (α_p , [$\mu\text{mol } \mu\text{mol}^{-1}$]), maximum net photosynthetic rate (P_{Nmax} , [$\mu\text{mol m}^{-2} \text{s}^{-1}$]), saturation irradiance (I_{sat} , [$\mu\text{mol m}^{-2} \text{s}^{-1}$]), light-compensation point (I_c , [$\mu\text{mol m}^{-2} \text{s}^{-1}$]), dark respiration rate (R_d , [$\mu\text{mol m}^{-2} \text{s}^{-1}$]), need electron numbers per assimilation a CO_2 molecule ($1/\theta$, [$\mu\text{mol } \mu\text{mol}^{-1}$]), need apparent electron numbers per assimilation a CO_2 molecule ($1/\theta_a$, [$\mu\text{mol } \mu\text{mol}^{-1}$]) and determination coefficient (R^2). All values indicate the mean \pm SE ($n = 3$) except for measured values. Significant differences of the means for three rice cultivars are indicated by *lowercase letters* ($p < 0.05$).

	JR3015		Wufengyou3015		Jifengyou3015	
	Fitted values	Measured values	Fitted values	Measured values	Fitted values	Measured values
α_p [$\mu\text{mol } \mu\text{mol}^{-1}$]	0.042 ± 0.011^b	-	0.070 ± 0.019^a	-	0.072 ± 0.012^a	-
P_{Nmax} [$\mu\text{mol m}^{-2} \text{s}^{-1}$]	17.48 ± 0.47^c	≈ 17.98	20.76 ± 0.57^b	≈ 20.99	26.30 ± 0.56^a	≈ 26.98
I_{sat} [$\mu\text{mol m}^{-2} \text{s}^{-1}$]	$1,223.98 \pm 25.45^c$	$\approx 1,200$	$1,425.36 \pm 35.59^b$	$\approx 1,500$	$1,771.08 \pm 34.14^a$	$\approx 1,800$
I_c [$\mu\text{mol m}^{-2} \text{s}^{-1}$]	15.61 ± 2.59^b	≈ 15	13.05 ± 2.23^b	≈ 13	23.01 ± 1.59^a	≈ 23
R_d [$\mu\text{mol m}^{-2} \text{s}^{-1}$]	0.62 ± 0.14^c	≈ 0.65	1.08 ± 0.27^b	≈ 1.10	1.66 ± 0.21^a	≈ 1.67
$1/\theta$ [$\mu\text{mol } \mu\text{mol}^{-1}$]	7.64 ± 0.32^a	-	4.61 ± 0.24^b	-	4.43 ± 0.28^b	-
$1/\theta_a$ [$\mu\text{mol } \mu\text{mol}^{-1}$]	6.22 ± 0.78^a	-	5.73 ± 0.71^a	-	4.83 ± 0.08^a	-
R^2	0.989 ± 0.004	-	0.985 ± 0.022	-	0.990 ± 0.003	-

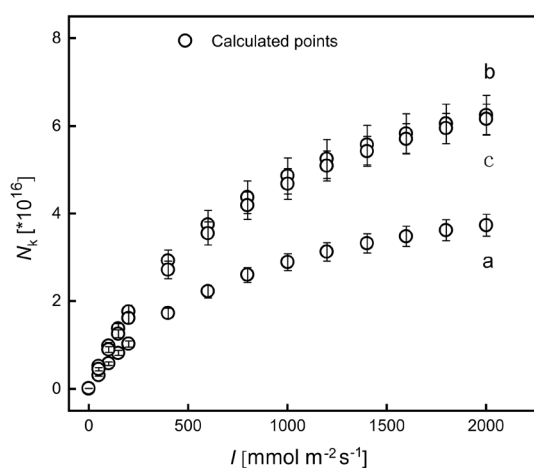


Fig. 3. Light-response curves of numbers of photosynthetic pigment molecules in the lowest state for three rice species (a – JR3015; b – Wufengyou3015; and c – Jifengyou3015). Values are means \pm standard errors ($n = 3$). N_k – numbers of photosynthetic pigment molecules in the excited state k ; I – light intensity.

of leaf function (Li *et al.* 2018). The ratio of chlorophyll a to b is usually between 2:1 and 3:1, and the size of this ratio can indicate the efficiency of the plant in utilizing different wavelengths of light and in electron transfer efficiency (Kang *et al.* 2022). In this study, we observed that although the chlorophyll content of JR3015 was almost half that of Wufengyou3015 and Jifengyou3015, the ratio of chlorophyll a to b was near the same for the three rice cultivars (Table 1). This suggests that the difference in J_{max} among the three rice cultivars cannot be explained by differences in their chlorophyll content alone, and may also be related to other physical features of the chlorophyll molecules in the three rice cultivars.

To answer the question addressed above, we introduced some intrinsic physical parameters (*e.g.*, σ_{ik} and τ_{min}) of photosynthetic pigment molecules that characterize the photosynthetic properties of a plant (Ye 2012, Ye

et al. 2013b). In this study, the σ_{ik} value of JR3015 was higher than that of Jifengyou3015 and Wufengyou3015. It indicated that photosynthetic pigment molecules of rice cultivar JR3015 still exhibited higher light energy capture abilities despite its lower chlorophyll content compared with the other two rice cultivars. Furthermore, the values of σ_{ik} for the three cultivars are about 10^{-21} m^2 (Table 1), which is similar to the results obtained by other methods (Ley and Mauzerall 1982, De Boni *et al.* 2007, Suggett *et al.* 2007). For example, Ley and Mauzerall (1982) estimated the value of the absorption cross-section of chlorophyll (σ_{chl}) of *Chlorella vulgaris* to be $2.90 (\pm 0.10) \times 10^{-21} \text{ m}^2$ by measuring the rates of O_2 production by cell suspensions illuminated with flashing light; De Boni *et al.* (2007) used white light continuum Z-scan technique to study the values of σ_{chl} of chlorophyll a extracted from spinach in the spectral range between 460 and 700 nm and found that the value of σ_{chl} was $\sim 4.7 \times 10^{-21} \text{ m}^2$ at 680 nm. Suggett *et al.* (2007) studied *Emiliania huxleyi* (Lohmann) using the fast repetition rate fluorescence technique; they found the value of σ_{chl} to be $3.25 \times 10^{-21} \text{ m}^2$ at low light intensity [$25 \mu\text{mol}(\text{photon}) \text{ m}^{-2} \text{ s}^{-1}$] and to be $2.95 \times 10^{-21} \text{ m}^2$ at high light intensity [$600 \mu\text{mol}(\text{photon}) \text{ m}^{-2} \text{ s}^{-1}$]. This indicates that the values of σ_{ik} obtained in this study are consistent with those of previous studies, confirming their magnitude to be approximately 10^{-21} m^2 .

τ_{min} of JR3015 was the smallest among the three rice cultivars (Table 1), indicating that its exciton transfer rate between photosynthetic pigments or between photosynthetic pigments and PSII was faster than those of Jifengyou3015 and Wufengyou3015. This property increased the rate of exciton transfer to PSII or neighbor photosynthetic pigments, thereby enhancing the utilization of excited energy (Kondo *et al.* 2017, Yang *et al.* 2020b, 2023; Ye *et al.* 2020). Therefore, in this study, the joint action of σ_{ik} and τ_{min} to some extent compensated for reductions in chlorophyll contents, leading to J_{max} of JR3015 to be $104.01 \mu\text{mol m}^{-2} \text{ s}^{-1}$, despite its chlorophyll content being only half that of Jifengyou3015 and Wufengyou3015. Thus, σ_{ik} and τ_{min} are two intrinsic physical parameters

which are interpreted as indicators of the light energy absorption ability of photosynthetic pigments and the exciton transfer ability between photosynthetic pigments and PSII, respectively.

Moreover, our results have shown that the N_k of Wufengyou3015 and Jifengyou3015 were higher than that of JR3015 (Fig. 3). The longer τ_{\min} and higher N_k indicated that exciton occupied the excited state for a longer time, and in turn, photosynthetic pigment molecules required more time to recapture light energy. Additionally, higher occupancy of photosynthetic pigment molecules at a higher energy level will extend their average lifetime in the excited state. Our studies further supported the previous results regarding the faster recovery of PSII from photoinhibition in sun-acclimated leaves compared to shade leaves (Barth *et al.* 2001, Zhao *et al.* 2021). This suggests that under saturation irradiance, N_k was greater (and τ_{\min} was much longer) (Yang *et al.* 2023). Furthermore, our study identified significant differences in N_k and τ_{\min} between the rice cultivars (Fig. 3, Table 1). Hence, our results (τ_{\min} , Table 1) support the conclusion reached by Murchie and Niyogi (2011) that the lifetime of the singlet state will be prolonged when light is excessive and excited chlorophyll pigments (N_k , Fig. 3) do not rapidly de-excite and engage in photochemistry or other energy dissipation pathways (e.g., fluorescence emission and heat dissipation).

Photosynthetic capacity: Values of $\theta = \alpha_p/\alpha_c$ derived from the $J-I$ and P_N-I curves enabled an intrinsic assessment of the total photosynthetic electron-use efficiency through PSII (Ye *et al.* 2013b). Despite J_{\max} being approximately 1.17-fold greater for Jifengyou3015 than for JR3015, $P_{N_{\max}}$ was about 1.5-fold greater for Jifengyou3015. This difference may be the reason why the photosynthetic electron-use efficiency of Jifengyou3015 ($\theta = \alpha_p/\alpha_c = 22.57\%$) was higher than that of JR3015 ($\theta = 13.08\%$). JR3015 required approximately 7.64 electrons per CO_2 molecule assimilation, whereas Jifengyou3015 needed only around 4.43 photosynthetic electrons. These findings further substantiate the positive correlation between lower PSII-mediated consumption of photosynthetic electrons and greater electron-use efficiency. Additionally, the non-uniformity of net CO_2 assimilation efficiency among cultivars and the cultivar-specific variation in utilization of energy/reductant for CO_2 uptake are emphasized compared to other assimilatory processes. Our findings revealed that the apparent electron count per CO_2 molecule assimilation was the highest for JR3015 and the lowest for Jifengyou3015, despite no significant difference in their values of $1/\theta_a$ among the three rice cultivars (Table 2, $p > 0.05$).

The size of stomatal conductance directly determines the supply of carbon dioxide and the rate of water transpiration, thereby affecting the rate of photosynthesis in plant leaves (Zhao *et al.* 2019). Although stomatal conductance does not directly affect the rate of electron transfer, the overall efficiency of photosynthesis and the ability to produce products indirectly impact the rate of electron transfer (Oue 2023). In the present study, the light response of stomatal conductance in three rice varieties

revealed that the maximum stomatal conductance of JR3015 was significantly lower than that of Wufengyou3015 and Jifengyou3015 (Table 1S, *supplement*; Fig. 1S, *supplement*). However, there was no significant difference in the maximum stomatal conductance between Wufengyou3015 and Jifengyou3015. Furthermore, there were no significant differences in J_{\max} among the three rice varieties (Table 2), indicating that stomatal conductance did not significantly correlate with the electron transport rate. Additionally, there were significant differences in the $P_{N_{\max}}$ among the three rice varieties (Table 1). Thus, the similar levels of maximum stomatal conductance and chlorophyll content in Wufengyou3015 and Jifengyou3015 cannot account for the significant differences in their $P_{N_{\max}}$, and the significant differences in stomatal conductance among the varieties cannot explain the similar levels of J_{\max} .

In summary, our results indicate that J depends not only on chlorophyll contents and σ_{ik} , but also on τ_{\min} . Additionally, photosynthetic electron-use efficiency and apparent photosynthetic electron-use efficiency *via* PSII played an important role in determining the numerical values of P_N and $P_{N_{\max}}$. Nevertheless, compared to the impact of chlorophyll content and stomatal conductance on P_N and $P_{N_{\max}}$, the present study did not exclude the influence of Rubisco amount or mesophyll conductance, which may also be major factors. In addition, the specific traits of photosynthetic pigment molecules that directly impact the numerical values of σ_{ik} , τ_{\min} , and θ are still unclear.

Conclusions: The mechanism of the relationship between photosynthetic capacity, chlorophyll content, and leaf light absorption ability was elucidated using intrinsic biophysical parameters as eigen-absorption cross-section (σ_{ik}) and the lowest minimum average lifetime of photosynthetic pigment molecules in the lowest excited state (τ_{\min}). We found significant differences between the three rice cultivars in chlorophyll content and maximum net photosynthetic rate ($P_{N_{\max}}$) but not in the maximum electron transport rate (J_{\max}). Our key finding is that JR3015 variety with lower leaf chlorophyll content can produce the similar electron transport rates as the other rice varieties with higher leaf chlorophyll content because the former had higher σ_{ik} and lower τ_{\min} . Higher σ_{ik} represented that the rice had high light absorption abilities of photosynthetic pigment molecules to produce more excitons, and lower τ_{\min} could accelerate the excited energy/excitons transfer to the photochemistry center to increase photosynthetic electron rates *via* photosystem II.

References

- Barth C., Krause G.H., Winter K.: Responses of photosystem I compared with photosystem II to high-light stress in tropical shade and sun leaves. – *Plant Cell Environ.* **24**: 163-176, 2001.
- Chandra R., Kang H.: Mixed heavy metal stress on photosynthesis, transpiration rate, and chlorophyll content in poplar hybrids. – *For. Sci. Technol.* **12**: 55-61, 2016.
- Chen M.: Chlorophyll modifications and their spectral extension in oxygenic photosynthesis. – *Annu. Rev. Biochem.* **83**: 317-340, 2014.

- Chen T., Chen Z., Atul P.S. *et al.*: Characterization of a novel gain-of-function spotted-leaf mutant with enhanced disease resistance in rice. – *Rice Sci.* **26**: 372-383, 2019.
- Chen X., Sun J., Lyu M. *et al.*: Prediction of photosynthetic light-response curves using traits of the leaf economics spectrum for 75 woody species: effects of leaf habit and sun–shade dichotomy. – *Am. J. Bot.* **108**: 423-431, 2021.
- Coleman H.D., Samuels A.L., Guy R.D., Mansfield S.D.: Perturbed lignification impacts tree growth in hybrid poplar – a function of sink strength, vascular integrity, and photosynthetic assimilation. – *Plant Physiol.* **148**: 1229-1237, 2008.
- De Boni L., Correa D.S., Pavinatto F.J. *et al.*: Excited state absorption spectrum of chlorophyll *a* obtained with white-light continuum. – *J. Chem. Phys.* **126**: 165102, 2007.
- Essemine J., Xiao Y., Qu M. *et al.*: Cyclic electron flow may provide some protection against PSII photoinhibition in rice (*Oryza sativa* L.) leaves under heat stress. – *J. Plant Physiol.* **211**: 138-146, 2017.
- Hitchcock A., Hunter C.N., Sobotka R. *et al.*: Redesigning the photosynthetic light reactions to enhance photosynthesis – the *PhotoRedesign* consortium. – *Plant J.* **109**: 23-34, 2022.
- Hu P., Ma J., Kang S.J. *et al.*: *Chlorophyllide-a oxygenase 1 (OsCAO1)* over-expression affects rice photosynthetic rate and grain yield. – *Rice Sci.* **30**: 87-91, 2023.
- Hu W., Tian S.B., Di Q. *et al.*: Effects of exogenous calcium on mesophyll cell ultrastructure, gas exchange, and photosystem II in tobacco (*Nicotiana tabacum* Linn.) under drought stress. – *Photosynthetica* **56**: 1204-1211, 2018.
- Hussain S., Iqbal N., Raza M.A. *et al.*: Distribution and effects of ionic titanium application on energy partitioning and quantum yield of soybean under different light conditions. – *Photosynthetica* **57**: 572-580, 2019.
- Insausti P., Ploschuk E.L., Izaguirre M.M., Podworny M.: The effect of sunlight interception by sooty mold on chlorophyll content and photosynthesis in orange leaves (*Citrus sinensis* L.). – *Eur. J. Plant Pathol.* **143**: 559-565, 2015.
- Kalisz A., Jezdinsky A., Pokluda R. *et al.*: Impacts of chilling on photosynthesis and chlorophyll pigment content in juvenile basil cultivars. – *Hortic. Environ. Biotech.* **57**: 330-339, 2016.
- Kang J.H., Yoon H.L., Lee J.M. *et al.*: Electron transport and photosynthetic performance in *Fragaria* × *ananassa* Duch. acclimated to the solar spectrum modified by a spectrum conversion film. – *Photosynth. Res.* **151**: 31-46, 2022.
- Kitao M., Yasuda Y., Kodani E. *et al.*: Integration of electron flow partitioning improves estimation of photosynthetic rate under various environmental conditions based on chlorophyll fluorescence. – *Remote Sens. Environ.* **254**: 112273, 2021.
- Kondo T., Chen W.J., Schlau-Cohen G.S.: Single-molecule fluorescence spectroscopy of photosynthetic systems. – *Chem. Rev.* **117**: 860-898, 2017.
- Ley A.C., Mauzerall D.C.: Absolute absorption cross-sections for photosystem II and the minimum quantum requirement for photosynthesis in *Chlorella vulgaris*. – *BBA-Bioenergetics* **680**: 95-106, 1982.
- Li Y., He N., Hou J. *et al.*: Factors influencing leaf chlorophyll content in natural forests at the biome scale. – *Front. Ecol. Evol.* **6**: 64, 2018.
- Lichtenthaler H.K.: Chlorophylls and carotenoids: pigments of photosynthetic biomembranes. – *Method. Enzymol.* **148**: 350-382, 1987.
- Major K.M., Dunton K.H.: Variations in light-harvesting characteristics of the seagrass, *Thalassia testudinum*: evidence for photoacclimation. – *J. Exp. Mar. Biol. Ecol.* **275**: 173-189, 2002.
- Mauro R.P., Occhipinti A., Longo A.M.G., Mauromicale G.: Effects of shading on chlorophyll content, chlorophyll fluorescence and photosynthesis of subterranean clover. – *J. Agron. Crop Sci.* **197**: 57-66, 2011.
- Mirkovic T., Ostroumov E.E., Anna J.M. *et al.*: Light absorption and energy transfer in the antenna complexes of photosynthetic organisms. – *Chem. Rev.* **117**: 249-293, 2017.
- Murchie E.H., Horton P.: Acclimation of photosynthesis to irradiance and spectral quality in British plant species: chlorophyll content, photosynthetic capacity and habitat preference. – *Plant Cell Environ.* **20**: 438-448, 2008.
- Murchie E.H., Niyogi K.K.: Manipulation of photoprotection to improve plant photosynthesis. – *Plant Physiol.* **155**: 86-92, 2011.
- Nilkens M., Kress E., Lambrev P. *et al.*: Identification of a slowly inducible zeaxanthin-dependent component of non-photochemical quenching of chlorophyll fluorescence generated under steady-state conditions in *Arabidopsis*. – *BBA-Bioenergetics* **1797**: 466-475, 2010.
- Oue H.: Comparisons of the stomatal conductance and electron transport rate of three Japanese rice cultivars including Himenorin in Ehime Prefecture. – *J. Agric. Meteorol.* **79**: 77-84, 2023.
- Porra R.J.: The chequered history of the development and use of simultaneous equations for the accurate determination of chlorophylls *a* and *b*. – *Photosynth. Res.* **73**: 149-156, 2002.
- Qian X., Liu L., Croft H., Chen J.: Relationship between leaf maximum carboxylation rate and chlorophyll content preserved across 13 species. – *J. Geophys. Res.-Biogeo.* **126**: e2020JG006076, 2021.
- Roháček K.: Chlorophyll fluorescence parameters: the definitions, photosynthetic meaning, and mutual relationships. – *Photosynthetica* **40**: 13-29, 2002.
- Ruban A.V.: Evolution under the sun: optimizing light harvesting in photosynthesis. – *J. Exp. Bot.* **66**: 7-23, 2015.
- Sanda S., Yoshida K., Kuwano M. *et al.*: Responses of the photosynthetic electron transport system to excess light energy caused by water deficit in wild watermelon. – *Physiol. Plantarum* **142**: 247-264, 2011.
- Sarkar R.K.: Saccharide content and growth parameters in relation with flooding tolerance in rice. – *Biol. Plantarum* **40**: 597-603, 1997.
- Silva M.D.A., Pincelli R.P., Barbosa A.D.M.: Water stress effects on chlorophyll fluorescence and chlorophyll content in sugarcane cultivars with contrasting tolerance. – *Biosci. J.* **34**: 75-87, 2018.
- Slattery R.A., VanLooke A., Bernacchi C.J. *et al.*: Photosynthesis, light use efficiency, and yield of reduced-chlorophyll soybean mutants in field conditions. – *Front. Plant Sci.* **8**: 549, 2017.
- Sofó A., Dichio B., Montanaro G., Xiloyannis C.: Photosynthetic performance and light response of two olive cultivars under different water and light regimes. – *Photosynthetica* **47**: 602-608, 2009.
- Suggett D.J., Le Floc'h E., Harris G.N. *et al.*: Different strategies of photoacclimation by two strains of *Emiliania huxleyi* (Haptophyta). – *J. Phycol.* **43**: 1209-1222, 2007.
- Tekalign T., Hammes P.S.: Response of potato grown under non-inductive condition paclobutrazol: shoot growth, chlorophyll content, net photosynthesis, assimilate partitioning, tuber yield, quality, and dormancy. – *Plant Growth Regul.* **43**: 227-236, 2004.
- Yang P., Li Y., He C. *et al.*: Phenotype and TMT-based quantitative proteomics analysis of *Brassica napus* reveals new insight into chlorophyll synthesis and chloroplast structure. – *J. Proteomics* **214**: 103621, 2020a.
- Yang X.L., Dong W., Liu L.H. *et al.*: Uncovering the differential

- growth of *Microcystis aeruginosa* cultivated under nitrate and ammonium from a pathophysiological perspective. – ACS ES&T Water 3: 1161-1171, 2023.
- Yang X.L., Liu L.H., Yin Z.K. *et al.*: Quantifying photosynthetic performance of phytoplankton based on photosynthesis–irradiance response models. – Environ. Sci. Eur. 32: 24, 2020b.
- Ye Z.-P.: Nonlinear optical absorption of photosynthetic pigment molecules in leaves. – Photosynth. Res. 112: 31-37, 2012.
- Ye Z.-P., Kang H.-J., An T. *et al.*: Modeling light response of electron transport rate and its allocation for ribulose biphosphate carboxylation and oxygenation. – Front. Plant Sci. 11: 581851, 2020.
- Ye Z.-P., Robakowski P., Suggett D.J.: A mechanistic model for the light response of photosynthetic electron transport rate based on light harvesting properties of photosynthetic pigment molecules. – Planta 237: 837-847, 2013a.
- Ye Z.-P., Suggett J.D., Robakowski P., Kang H.-J.: A mechanistic model for the photosynthesis-light response based on the photosynthetic electron transport of photosystem II in C₃ and C₄ species. – New Phytol. 199: 110-120, 2013b.
- Zhang Z., Li G., Gao H. *et al.*: Characterization of photosynthetic performance during senescence in stay-green and quick-leaf-senescence *Zea mays* L. inbred lines. – PLoS ONE 7: e42936, 2012.
- Zhao N., Meng P., Yu X.: Photosynthetic stimulation of saplings by the interaction of CO₂ and water stress. – J. Forestry Res. 30: 1233-1243, 2019.
- Zhao X., Chen T., Feng B. *et al.*: Non-photochemical quenching plays a key role in light acclimation of rice plants differing in leaf color. – Front. Plant Sci. 7: 1968, 2017.
- Zhao Y., Zou Y., Wang L., Wang C.: Tropical rainforest successional processes can facilitate successfully recovery of extremely degraded tropical forest ecosystems following intensive mining operations. – Front. Environ. Sci. 9: 701210, 2021.

Appendix 1. Definitions of the abbreviations.

Abbreviation	Definition	Units
d	Thickness of the leaf sample	m
g_i	Degeneracy of energy level of photosynthetic pigment molecules in the ground state (i)	dimensionless
g_k	Degeneracy of energy level of photosynthetic pigment molecules in the excited state (k)	dimensionless
I	Light intensity	$\mu\text{mol}(\text{photon})\text{ m}^{-2}\text{ s}^{-1}$
I_c	Light-compensation point	$\mu\text{mol}(\text{photon})\text{ m}^{-2}\text{ s}^{-1}$
I_{sat}	Saturation light intensity corresponding to maximum net photosynthetic rate	$\mu\text{mol m}^{-2}\text{ s}^{-1}$
J	Electron transport rate	$\mu\text{mol m}^{-2}\text{ s}^{-1}$
$J-I$	Light-response curve of photosynthetic electron transport rate	
J_{max}	Maximum photosynthetic electron transport rate	$\mu\text{mol m}^{-2}\text{ s}^{-1}$
N_k	Numbers of photosynthetic pigment molecules in the excited state k	
N_0	Total photosynthetic pigment molecules of the measured leaf sample	
n_0	Number of photosynthetic pigment molecules of the measured leaf sample per unit volume	m^{-3}
P_N	Net photosynthetic rate	$\mu\text{mol m}^{-2}\text{ s}^{-1}$
PAR_{sat}	Saturation irradiance corresponding to maximum electron transport rate	$\mu\text{mol m}^{-2}\text{ s}^{-1}$
P_N-I	Light-response curve of photosynthesis	
$P_{N\text{max}}$	Maximum net photosynthetic rate	$\mu\text{mol m}^{-2}\text{ s}^{-1}$
R_d	Mitochondrial CO ₂ release in the dark	$\mu\text{mol m}^{-2}\text{ s}^{-1}$
S	Measured area of the leaf sample	m^2
α_a	The slope of the linear part of the light-response curve in weak photosynthetic flux density between 0 and 150 $\mu\text{mol}(\text{photon})\text{ m}^{-2}\text{ s}^{-1}$	$\mu\text{mol}\mu\text{mol}^{-1}$
α_c	Initial slope of the light-response curve of electron transport rate	$\mu\text{mol}\mu\text{mol}^{-1}$
α_p	Initial slope of photosynthesis–irradiance response	$\mu\text{mol}\mu\text{mol}^{-1}$
α'	Fraction of light absorbed by PSII	dimensionless
β_c	Coefficient of dynamic downregulation for PSII/photoinhibition of the light-response curve of photosynthetic electron transport rate	$\mu\text{mol}(\text{photon})^{-1}\text{ m}^2\text{ s}$
β_p	Coefficient of dynamic downregulation for PSII/photoinhibition of the light-response curve of photosynthesis	$\mu\text{mol}(\text{photon})^{-1}\text{ m}^2\text{ s}$
β'	Leaf absorptance	dimensionless
γ_e	Saturation coefficient of the light-response curve of photosynthetic electron transport rate	$\mu\text{mol}(\text{photon})^{-1}\text{ m}^2\text{ s}$
γ_p	Saturation coefficient of the light-response curve of photosynthesis	$\mu\text{mol}(\text{photon})^{-1}\text{ m}^2\text{ s}$
φ	Exciton-use efficiency in PSII	dimensionless
σ_{ik}	Eigen-absorption cross-section of photosynthetic pigment molecule from ground state i to excited state k due to light illumination	m^2
θ	Electron-use efficiency via PSII	$\mu\text{mol}\mu\text{mol}^{-1}$
τ_{min}	Minimum average lifetime of photosynthetic pigment molecules in the excited state	s

© The authors. This is an open access article distributed under the terms of the Creative Commons BY-NC-ND Licence.